THE JOURNAL OF PHYSICAL CHEMISTRY A
A JOURNAL OF THE AMERICAN CHEMICAL SOCIETY

pubs.acs.org/JPCA Article

Monomers of Glycine and Serine Have a Limited Ability to Hydrate in the Atmosphere

Published as part of The Journal of Physical Chemistry virtual special issue "125 Years of The Journal of Physical Chemistry".

Benjamin T. Ball, Sara Vanovac, Tuguldur T. Odbadrakh, and George C. Shields*

Cite This: *J. Phys. Chem. A* 2021, 125, 8454–8467 Read Online

ACCESS | Metrics & More | Article Recommendations | Supporting Information

ABSTRACT: The role of atmospheric aerosols on climate change is one of the biggest uncertainties in most global climate models. Organic aerosols have been identified as potential cloud condensation nuclei (CCN), and amino acids are organic molecules that could serve as CCN. Amino acids make up a significant portion of the total organic material in the atmosphere, and herein we present a systematic study of hydration for two of the most common atmospheric amino acids, glycine and serine. We compute DLPNO/CCSD(T)//M08-HX/MG3S thermodynamic properties and atmospheric concentrations of $Gly(H_2O)_n$ and $Ser(H_2O)_n$, where n = 1−5. We predict that serine−water clusters have higher concentrations at n = 1 and 5, while glycine−water clusters have higher concentrations at n = 2−4. However, both glycine and serine are inferred to exist primarily in their nonhydrated monomer forms in the absence of other species such as sulfuric acid.

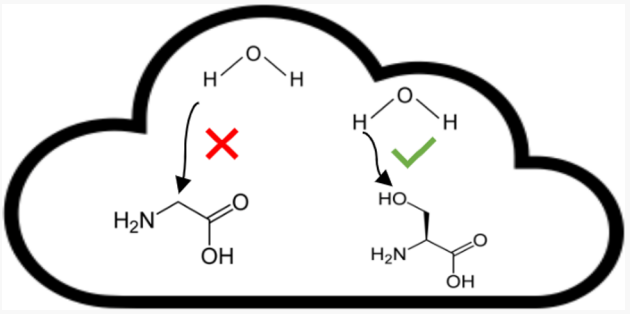

INTRODUCTION

The role of atmospheric aerosols on climate change is one of the biggest uncertainties in most global climate models. Aerosols and clouds are thought to have a net cooling effect, but the extent of this cooling is still debated, and more research is needed to reach definitive conclusions. Numerous studies have identified sulfates to be the primary molecules that play a key role in the formation of cloud condensation nuclei (CCN), but organic aerosols have also been identified as potential CCN.[1] Amino acids are organic molecules that could serve as CCN, and interest in their involvement in atmospheric aerosols has grown in the recent past.[2−6] Amino acids offer both hydrogen-bond donor and acceptor sites through their carboxylic acid group and amine group, allowing for the bidirectional growth of clusters. Additionally, the role of free amino acids in the formation of prebiotic polypeptides before the advent of ribosomes is being explored within the context of gas-phase clusters and aerosol particles.[7−11] In all of these studies, the interaction of amino acids with water molecules and its consequences are the main focus due to the ubiquitous nature of water. Quantum chemistry methods have been applied to understanding new particle formation and heterogeneous processes, and recently the focus has shifted toward the role of amino acids in this context.[12]

The sources of amino acids are numerous and varied, with the Miller experiment as perhaps the foundational study of amino acid synthesis.[13,14] Since then, amino acids have been observed in extraterrestrial objects such as meteorites and the atmospheres of different planets.[15−17] On earth, atmospheric measurements have also established the presence of both free amino acids and their polypeptide polymeric forms.[18−22] Amino acids can enter atmospheric aerosols in one of two ways, as primary aerosols or secondary aerosols. In primary aerosols, amino acids are introduced into the atmosphere already embedded in an aerosol, while for secondary aerosols, amino acids begin in the gas phase and become aerosols through a gas-to-particle conversion.[23] With many sources, amino acids now make up a significant portion of the total organic material in the atmosphere, and their interactions with water have been studied, including glycine[24−37] and serine.[38−47] However, these studies of the gas-phase conformations and microsolvation of amino acids have focused on spectroscopic properties and the electronic potential energy surface (PES) under vacuum conditions. Given that most atmospheric amino acids exist in solution in the aerosol phase, their potential role in the formation of CCN starting from gas-phase free monomers is incompletely understood and presents a gap in

Received: June 21, 2021
Published: September 16, 2021

https://doi.org/10.1021/acs.jpca.1c05466
J. Phys. Chem. A 2021, 125, 8454−8467

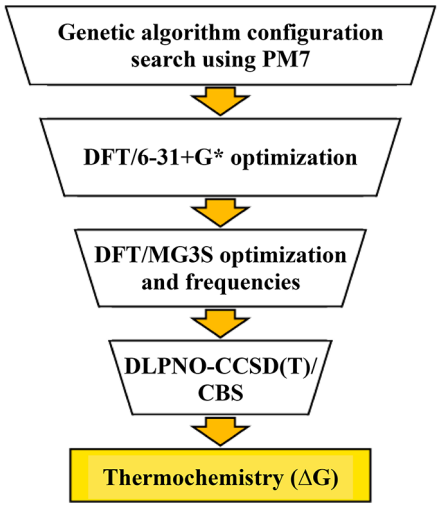

Figure 1. Schematic of the methodology used to identify minimum-energy structures and to compute their thermodynamic properties.

the CCN formation model. In this article, we present a systematic study of the Gibbs free energy surface of gas-phase clusters of $Gly(H_2O)_{n=0-5}$ and $Ser(H_2O)_{n=0-5}$ in order to explore the effects of varying functional groups on the formation of hydrated clusters under atmospheric conditions. We hypothesize that the added flexibility and hydrogen bonding site associated with serine's CH_2OH functional group would have a significant stabilizing effect on water clusters, leading to easier hydration of serine than glycine in the atmosphere. In this pursuit, one of the most challenging tasks is to thoroughly explore the configurational space of the hydrated amino acid clusters in order to identify stable low-energy clusters. We now describe our computational methodology, followed by the results and discussion.

METHODOLOGY

Conformational Analysis of the Isolated Amino Acids. Our methodology for the configurational analysis of hydrated amino acids requires a preliminary exploration of the conformational space of the isolated amino acids so that accurate monomer geometries can be used as starting guess structures. To this end, we employed an automated conformational search algorithm based on meta-dynamics developed by Grimme et al. called CREST.[48,49] This method uses the GFn2-XTB self-consisted tight-binding model to compute energies and a combination of meta-dynamics and a genetic *z*-matrix crossing to explore the conformational space of a molecule to identify low-energy conformers and rotamers. The meta-dynamics simulation applies a biasing potential to "fill up" previously accessed minima on the GFn2-XTB PES in order to drive the system toward other inaccessible minima regardless of barrier heights. The genetic *z*-matrix crossing generates new structures

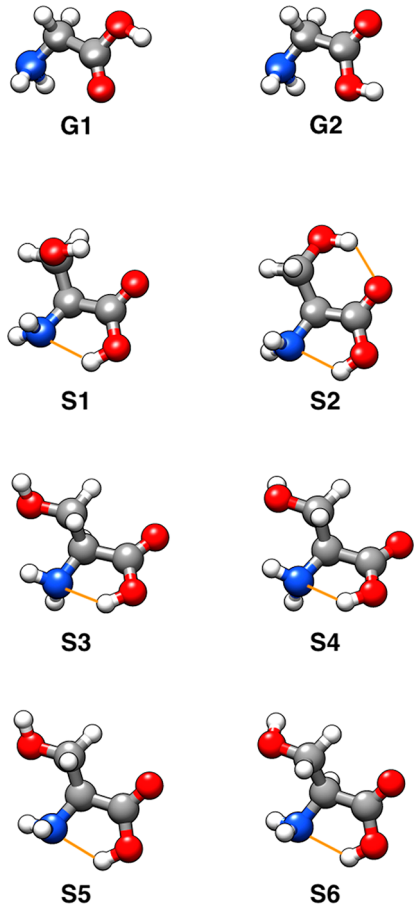

Figure 2. Conformers of monomeric glycine (G1-G2) and serine (S1-S6) within 2 kcal mol^{-1} of the 298 K global minimum DLPNO-CCSD(T)/CBS//M08-HX/MG3S Gibbs free energy minimum, G1 and S1. Intramolecular hydrogen bonds are marked using orange lines. Intermolecular hydrogen bonds are defined as having a bond length of less than 2.2 Å and a bond angle of between 140 and 180°. Intramolecular hydrogen bonds have different criteria; each intramolecular bond angle ranges from 120 to 130° and has a bond length of less than 2.2. Å.

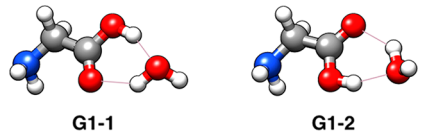

Figure 3. $Gly(H_2O)$ clusters within 2 kcal mol^{-1} of the ΔG°_{298} DLPNO-CCSD(T)/CBS//M08-HX/MG3S global minimum, G1-1. G1-1 is the ΔE_{el} DLPNO-CCSD(T) and ΔE_{el} and ΔG°_{298} M08-HX global minimum energy structure as well.

Table 1. DLPNO-CCSD(T)/CBS//ωB97xD/6-31++G Gibbs Free Energies of Formation Relative to the DLPNO-CCSD(T)/CBS//M08-HX/MG3S Values for the Global Minima of $Gly(H_2O)$ (G1-1) and $Gly(H_2O)_5$ (G5-1) in Units of kcal mol^{-1}[a]**

		ΔΔG (kcal/mol)			
theory	cluster	0 K	216.65 K	273.15 K	298.15 K
ωB97xD/MG3S	G1-1	−0.10	−0.12	−0.12	−0.12
	G5-1	−0.79	0.16	0.40	0.51
ωB97xD/6-311++G**	G1-1	−0.02	−0.09	−0.10	−0.10
	G5-1	−0.75	0.58	0.82	0.94

[a]See the figures for structures.

https://doi.org/10.1021/acs.jpca.1c05466
J. Phys. Chem. A 2021, 125, 8454−8467

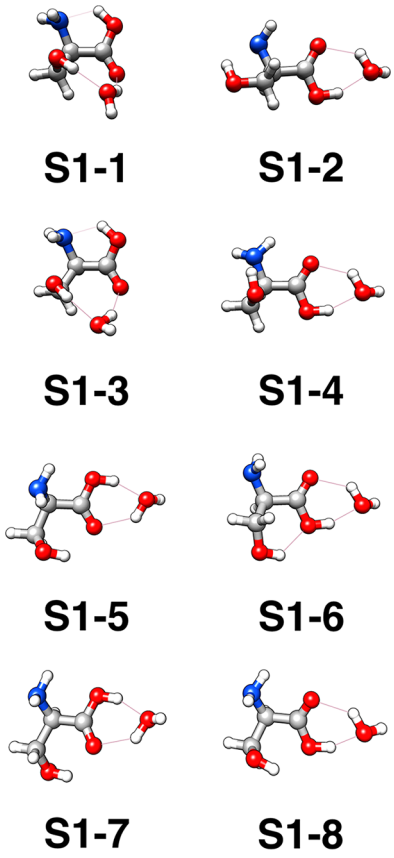

Figure 4. Ser(H_2O) clusters within 2 kcal mol^{-1} of the ΔG°_{298} DLPNO-CCSD(T)/CBS//M08-HX/MG3S global minimum, S1-1. S1-1 is also the ΔE_{el} global minimum structure according to DLPNO-CCSD(T), while S1-3 is the M08-HX ΔG°_{298} and ΔE_{el} global minimum structure.

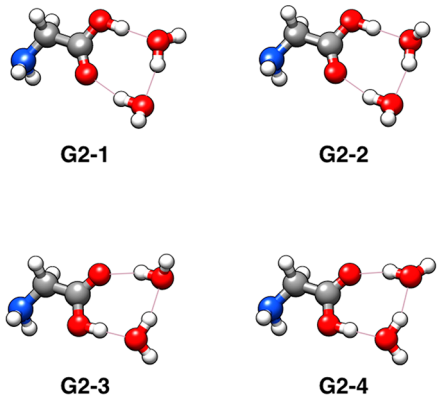

Figure 5. Gly$(H_2O)_2$ clusters within 2 kcal mol^{-1} of the ΔG°_{298} DLPNO-CCSD(T)/CBS//M08-HX/MG3S global minimum, G2-1. G2-1 is the ΔE_{el} DLPNO-CCSD(T) and ΔE_{el} and ΔG°_{298} M08-HX global minimum structure as well.

by projecting known geometries onto new geometries, thereby retaining frequently occurring motifs. The glycine and serine monomers were subject to this treatment, and their low-energy conformers within 6 kcal mol^{-1} of the global electronic energy minimum were retained for thermodynamic analysis. The further refinement of these geometries and computation of their thermodynamic properties follow the same procedure as described in detail in the next section. Finally, the free-energy minimum structures of glycine and serine were used in the subsequent investigation of their hydration.

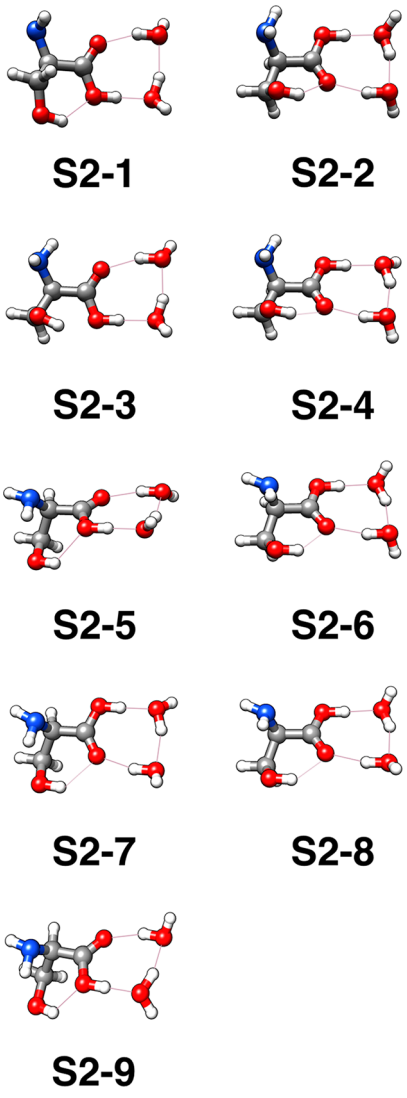

Figure 6. Ser$(H_2O)_2$ clusters within 2 kcal mol^{-1} of the ΔG°_{298} DLPNO-CCSD(T)/CBS//M08-HX/MG3S global minimum, S2-1. S2-2 is the ΔE_{el} DLPNO-CCSD(T) global minimum and the ΔG°_{298}M08- HX global minimum. Note that the ΔE_{el} M08-HX global minimum structure is not shown because it did not fall within 2 kcal mol^{-1} of our ΔG°_{298}DLPNO global minimum, illustrating the importance of not relying solely on DFT energies to determine ΔG°_T quantities.

Configurational Analysis of the Microsolvated Amino Acids. The configurational space of the hydrated amino acid clusters were explored using a genetic algorithm implemented in the OGOLEM program.[50] OGOLEM has previously been used in global optimizations of gas-phase clusters,[51−53] surface-bound clusters,[54,55] and molecular switches.[56] For each n number of water molecules (n = 1−5), a pool of 500 amino acid−water ($AA(H_2O)_n$) clusters were randomly generated from the lowest-energy conformers of the monomers, and the PM7[57] semi-empirical method was used to optimize each cluster's geometry.[58] This yielded an initial pool of local minimum-energy clusters on the PM7 PES. The evolutionary algorithm then proceeded in an iterative process as follows. A random pair of geometries were spliced in half, and the halves were exchanged to generate a new pair of geometries which were then optimized to the nearest minimum on the PES. Then a fitness function was used to determine whether the new geometries would replace the old

https://doi.org/10.1021/acs.jpca.1c05466
J. Phys. Chem. A 2021, 125, 8454−8467

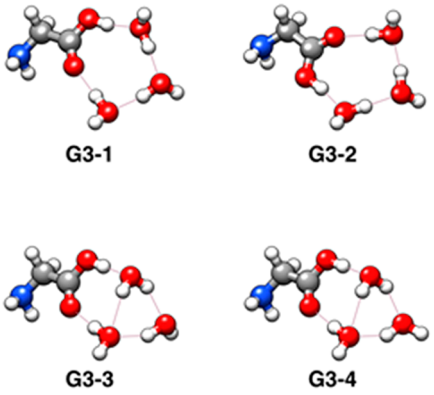

Figure 7. $Gly(H_2O)_3$ clusters within 2 kcal mol^{-1} of the $\Delta G°_{298}$ DLPNO-CCSD(T)/CBS//M08-HX/MG3S global minimum, G3-1. G3-1 is the ΔE_{el} DLPNO-CCSD(T) and the $\Delta G°_{298}$ M08-HX energy global minimum structure as well. G3-3 is the ΔE_{el}M08-HX global minimum energy structure.

geometries based on the structures' energies and motifs. This process was repeated until no new structures were found or a maximum of 20 000 iterations was reached. We eliminated duplicate structures from the final set of PM7 geometries using a combination of rotational constants and energies.

At this point, the validity of the PM7 PES should be discussed. The semiempirical nature of PM7 means that it retains quantum mechanical behavior while avoiding the high computational costs of quantum chemistry methods. It is known that PM7 overestimates binding energies as a result of a poor description and parametrization of noncovalent interactions; however, it gives acceptable geometries.[59] Furthermore, PM7 has been successfully applied to the study of enzymatic catalysis involving specific amino acid functional groups.[60] Given these issues, we are considering new methods for use in the first step of our methodology, such as DFTB+[61] and GFn2-XTB[48] tight-binding methods. In any case, we avoid bias from the PM7 PES by reoptimizing all PM7 structures at a density functional theory (DFT) level. We also performed the same configurational search for the zwitterionic form of each amino acid independently in order to include the charge-separated forms of the amino acids in the overall search. Ultimately, the final combined set of the canonical and zwitterionic forms of the PM7 minimum-energy structures was subject to reoptimization at the DFT level in the next step.

Each set of PM7 geometries was then optimized at the M08-HX[62]/6-31+G*[63−67] level of theory using the Gaussian 16 Rev B.01[68] program, and the rotational constants and energies were used to eliminate duplicate structures. Next, the M08-HX/MG3S level of theory was used to optimize the M08-HX/6-31+G* structures, further reducing the number of unique structures while improving the quantum mechanical description of the system. Finally, the structures were optimized one more time with much tighter convergence criteria and a denser integration grid, and their harmonic vibrational frequencies were computed. The harmonic frequencies of the clusters were used to compute the thermodynamic corrections to the electronic energies using the THERMO.PL[69] script from the National

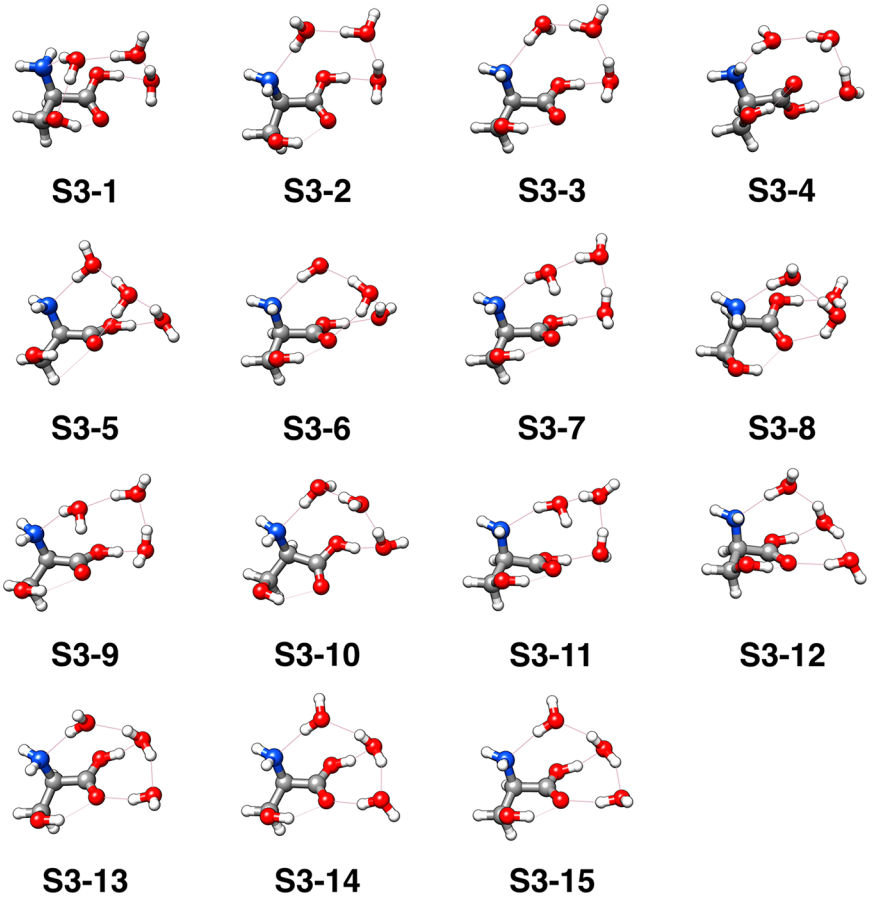

Figure 8. $Ser(H_2O)_3$ clusters within 2 kcal mol^{-1} of the $\Delta G°_{298}$ DLPNO-CCSD(T)/CBS//M08-HX/MG3S global minimum, S3-1. S3-1 is the ΔE_{el} DLPNO-CCSD(T) and ΔE_{el} and $\Delta G°_{298}$M08-HX global minimum structure as well.

https://doi.org/10.1021/acs.jpca.1c05466
J. Phys. Chem. A 2021, 125, 8454−8467

Institute of Standards and Technology. Finally, the DFT electronic energies of the clusters were corrected using the domain localized pair natural orbital coupled cluster DLPNO-CCSD(T)/cc-pVnZ (n = D,T,Q) level of theory implemented in the ORCA 4.2.1[70,71] program. The three electronic energies at the D, T, and Q levels were then used to compute the complete basis set (CBS) extrapolation of the electronic energy using the 4-5 inverse polynomial method.[72] Our previous works have shown that the 4-5 inverse polynomial extrapolation method yields acceptable electronic energies.[8,73,74] The DLPNO-CCSD-(T)/CBS electronic energies were then combined with the M08-HX/MG3S thermodynamic corrections to compute the Gibbs free energies of formation of $Gly(H_2O)_{n=1-5}$ and $Ser(H_2O)_{n=1-5}$ at 216.65, 273.15, and 298.15 K. We note here that for the hydrated amino acid systems all reported values correspond to the energy change associated with the reaction, bringing infinitely separated monomers to the bound geometry:

$$AA + nH_2O \leftrightarrow AA(H_2O)_n \quad (1)$$

The sequential Gibbs free energies of hydration were then used to estimate the atmospheric concentrations of $Gly(H_2O)_{n=0-5}$ and $Ser(H_2O)_{n=0-5}$ at these temperatures.[75] A schematic of the entire process is shown in Figure 1.

Validation of the Choice of Ab Initio Methods. The use of DFT geometries and thermal corrections along with DLPNO-CCSD(T) electronic energies has been used extensively in recent studies of atmospheric aerosols due to the favorable computational cost of the DLPNO-CCSD(T) method.[76] This is because the electronic energy contribution to the partition function is by far the largest contribution compared to the vibrational and rotational contributions.[77−79] Furthermore, the applicability of the DLPNO-CCSD(T) electronic structure on the DFT PES has been called into question. Therefore, we compared the M08-HX/MG3S level of theory in our procedure for the most popular density functional for hydrogen-bonded clusters, ωB97xD, using the MG3S and 6-311++G**[65,67,80−82] basis sets in order to investigate the effects of different PES's on the overall Gibbs free energy of formation when combined with their corresponding DLPNO-CCSD(T)/CBS electronic energies. The MG3S basis set is a truncated version of the Pople 6-311++G** basis set and is particularly suited to the M08-HX density functional with geometry optimizations.[62] Table 1 lists the Gibbs free energy of formation for the global free energy minima of $Gly(H_2O)$ (G1-1) and $Gly(H_2O)_5$ (G5-1) relative to their M08-HX/MG3S counterpart in units of kcal mol^{-1}. The data shows that for smaller clusters the ωB97xD functional has a lower formation energy while for larger clusters it has higher formation energies. Nevertheless, the differences are within 1 kcal mol^{-1}, which shows that the geometry and thermal corrections are within the chemical accuracy between the two density functionals when their electronic energies are corrected with DLPNO-CCSD(T)/CBS values.

RESULTS AND DISCUSSION

Conformations of Glycine and Serine. Before investigating the configurational space of the hydrated Gly and Ser clusters, we located the lowest-energy conformations of the serine and glycine monomers. In the case of glycine, we found that a conformer with no intramolecular hydrogen bonds should be the global ΔG°_{298} minimum in the gas phase, and this structure is confirmed in the literature as well.[31,83,84] As for serine, the trans conformer where the carboxyl hydrogen points toward the nitrogen of the amine group should be the global ΔG°_{298} minimum in the gas phase; this structure has also been identified in the literature.[40] Indeed, we have found the same global minima found previously by other researchers and present all of the DLPNO-CCSD(T)/CBS//M08-HX/MG3S minima within 2 kcal mol^{-1} of global ΔG°_{298} minimum structures G1 and S1 in Figure 2. Structures G1 and S1 were used in subsequent configurational sampling steps with added waters. The lowest-energy serine monomers all possess an intramolecular hydrogen bond. We define an intermolecular hydrogen bond as having a hydrogen bond length of less than 2.2 Å and a bond angle of between 140 and 180°. Intramolecular hydrogen bonds, depicted in Figure 2, all have bond lengths of about 2 Å and bond angles of between 121 and 123°. These intramolecular hydrogen bonds can be considered to be weak hydrogen bonds or van der Waals interactions. Only S2 has two intramolecular hydrogen bonds.

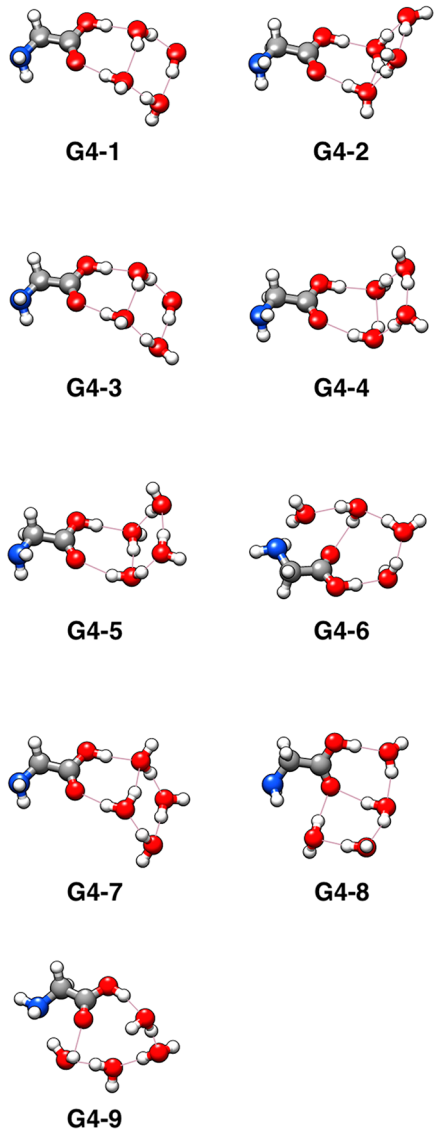

Figure 9. $Gly(H_2O)_4$ clusters within 2 kcal mol^{-1} of the ΔG°_{298} DLPNO-CCSD(T)/CBS//M08-HX/MG3S global minimum, G4-1. G4-2 is the ΔE_{el} DLPNO-CCSD(T) and the ΔG°_{298} M08-HX energy global minimum structure. G4-6 is the ΔE_{el}M08-HX global minimum energy structure.

Hydrated Clusters. We now turn our attention to the hydrated cluster configurations that are within 2 kcal mol^{-1} of

https://doi.org/10.1021/acs.jpca.1c05466
J. Phys. Chem. A 2021, 125, 8454−8467

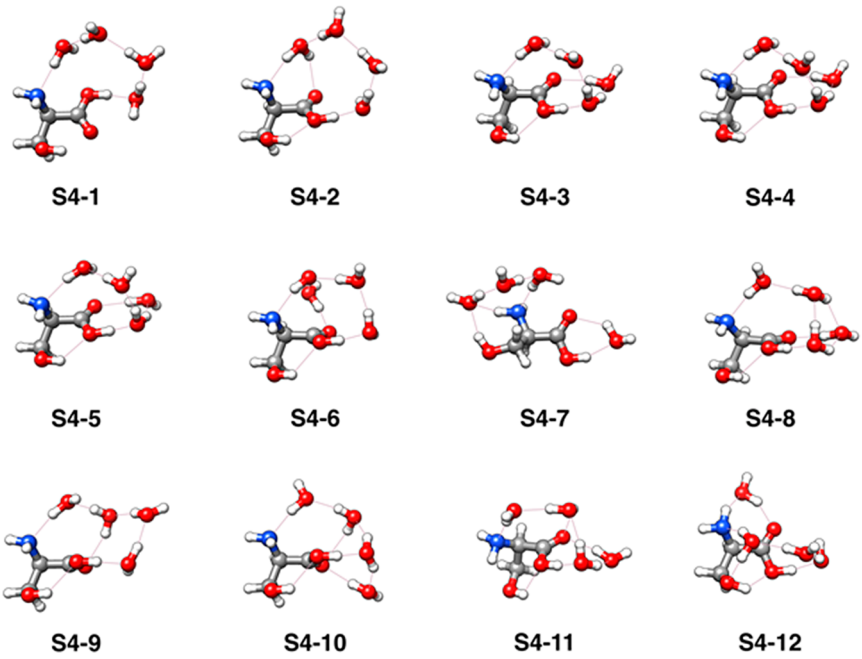

Figure 10. $Ser(H_2O)_4$ clusters within 2 kcal mol^{-1} of the ΔG°_{298} DLPNO-CCSD(T)/C BS//M08-HX/MG3S global minimum, S4-1. S4-5 is the ΔE_{el} DLPNO-CCSD(T) energy global minimum structure. The ΔG°_{298} and ΔE_{el} M08-HX global minimum structure is not shown because it does not fall within 2 kcal mol^{-1} of our ΔG°_{298} DLPNO-CCSD(T) global minimum. This illustrates the uneven performance of DFT methods for free-energy calculations.

the global minimum at each hydration level. At n = 1, glycine offers only its carboxyl group for strong hydrogen bonding while serine has an additional side chain (OH) group which can potentially bind a water molecule. Indeed, only two configurations of $Gly(H_2O)$ were found, as shown in Figure 3, while eight configurations of $Ser(H_2O)$, as shown in Figure 4, were identified. The lowest ΔG°_{298} energy structure for $Gly(H_2O)$ (G1-1) is in good agreement with configurations presented in previous studies, and nearly identical structures have been presented by Elm et al.,[2] Espinoza et al.,[30] Kishimoto,[31] and Bachrach.[27] In fact, Bachrach has reported low-energy configurations similar to ours for the systems $Gly(H_2O)_{1-4}$.[27] The global minimum ΔG°_{298} energy structure S1-1 has the water molecule forming a hydrogen-bonding bridge between the side chain and carboxyl group.[41] In this structure, the carboxyl group also forms a weak intramolecular hydrogen bond with the amine group, maximizing the number of hydrogen bonds. The lowest-energy structure for $Ser(H_2O)$ found by Chopra et al.[39] does not match our lowest-energy structure (Figure 4, S1-1); in their structure, water bridges the carboxyl OH to the amine nitrogen, while in our structure the water bridges the carboxyl double-bonded O to the hydroxymethyl side chain. Because OH−H hydrogen bonds are stronger than OH−N hydrogen bonds, the structures where a water bridges the hydroxyl side chain of serine with the carboxylic acid are more favorable than those where the water bridges the carboxylic acid and amine moieties of serine. We found structures with similar structural motifs to those presented by Chopra et al., but they were 7 kcal/mol higher than our ΔE_{el} M08-HX global minimum energy structure. This difference illustrates the importance of adequate configurational sampling.

For n = 2, the carboxyl group of both glycine and serine forms two hydrogen bonds to make a motif similar to the water tetramer. Four such clusters exist within 2 kcal mol^{-1} of the global minimum for glycine and nine for serine. Figures 5 and 6 show these cluster geometries. In all cases, each water molecule is in the hydrogen bond acceptor−donor (AD) configuration. The intramolecular hydrogen bond of serine between its amine and carboxyl groups (Figure 2) has been disrupted by the water molecules and are no longer present. However, a new intramolecular hydrogen bond between the side chain and the OH of the carboxyl group is displayed. Here, the side-chain oxygen atom is in the donor position while the carboxyl OH oxygen atom accepts the hydrogen bond. While our lowest-energy $Ser(H_2O)$ cluster (S1-1) matches the lowest-energy $Ser(H_2O)$ found by Jeon et al.,[41] our lowest-energy $Ser(H_2O)_2$ cluster (S2-1) does not. The cluster reported by Jeon et al.[41] for $Ser(H_2O)_2$ has the two water molecules bridging the carboxyl group to the side chain, and this discrepancy between their structure and ours can be attributed to a lack of thorough configurational sampling methods.

We note that the ΔE_{el} global minimum structure at the M08-HX level is not shown in Figure 6 because it did not fall within 2 kcal mol^{-1} of our ΔG°_{298} DLPNO global minimum, illustrating the importance of not relying solely on DFT energies to determine ΔG°_T quantities.[85−89]

At n = 3, the water molecules bind differently between glycine and serine, as shown in Figures 7 and 8. The glycine global minimum energy geometry (G3-1) has four hydrogen bonds, with each water molecule accepting one and donating one to form a pseudopentagon with the carboxyl group. A different motif of one acceptor−donor−donor (ADD) water, one acceptor-acceptor−donor (AAD) water, and one AD water exists at higher energies. In contrast, the flexibility of the additional side chain of serine allows for the formation of a 3D hydrogen bond network where the amine group participates. The global minimum energy configuration (S3-1) has one ADD water molecule bridging the amine NH_2 and side-chain OH groups and two AD water molecules connecting it to the OH of the carboxyl group. This $Ser(H_2O)_3$ is different from

https://doi.org/10.1021/acs.jpca.1c05466
J. Phys. Chem. A 2021, 125, 8454−8467

those previously found in the literature. Yanase et al. report a structure where two water molecules bridge the carboxyl to the amine nitrogen, while the third water bridges the amine nitrogen to the side chain. The focus of their work was interactions of the water molecule with the amino group of serine, so they considered only structures where water was located near the NH_2 group.[37]

For n = 4, the global ΔG°_{298} minimum of $Ser(H_2O)_4$ (S4-1), the water molecules form a ring-like structure bridging the OH group of the carboxyl to the amine NH_2 through a series of four AD waters. This same ring-like motif can be seen in the second-lowest-energy structure in the $Ser(H_2O)_3$ system (S3-2) and other higher-energy conformations. Compared to the $Ser(H_2O)_4$ system, the $Gly(H_2O)_4$ system has more uniform structures with fewer variations in geometries. The global minimum structure of the $Gly(H_2O)_4$ system (G4-1) creates a "pseudo-book" structure with six hydrogen bonds, where the "book" structure is an especially stable configuration of six water molecules at 298 K.[90,91] Here, the carboxyl OH and double-bonded O serve the same purpose as two water molecules in the actual six water book structure. The carboxyl OH hydrogen bonds to an acceptor−donor−donor (ADD) water while the carboxyl O hydrogen bonds to an acceptor−acceptor−donor (AAD) water molecule. Both of these AAD and ADD water molecules form hydrogen bonds with each other and then hydrogen bond to one of the two remaining AD water molecules. Higher-energy $Gly(H_2O)_4$ structures form a pentagon shape similar to those seen in the lower-energy $Gly(H_2O)_3$ structures, but with a fourth water molecule extending to form a weak interaction with the amine NH_2. These structures and other configurations within 2 kcal mol^{-1} are shown in Figures 9 and 10.

For n = 5, structures in the S5 system, Figures 11 and 12, form more intricate three-dimensional structures than the n = 1−3 systems. At the global minimum for $Ser(H_2O)_5$(S5-1), there are two major structural motifs. The first is a ring of three water molecules that serve to bridge the carboxyl O to the carboxyl OH group with two AD waters and one ADD water. This ADD water also begins the second structural motif, where the OH of the carboxyl is bridged through hydrogen bonding to the NH_2 by another ring-like structure of three waters. This second structural motif is similar to the lowest-energy $Ser(H_2O)_4$ structure (S4-1) and multiple low-energy structures found in the $Ser(H_2O)_3$ system (S3-2, S3-3, S3-4, etc.). A weak intramolecular hydrogen bond also occurs between the hydroxymethyl side chain and the carboxyl OH.

Compared to the $Ser(H_2O)_5$ system, the structures for $Gly(H_2O)_5$ tend to be more similar to one another with less variation as shown in Figure 11. The global minimum for the $Gly(H_2O)_5$ system (G5-1) creates a cube or box-like structure with six hydrogen bonds between three AD water molecules, one AAD water molecule, and one acceptor-only water molecule. Higher-energy structures within the $Gly(H_2O)_5$ system all have similar box-like structures but differ in the amount of hydrogen bonding and the connectivity of those hydrogen bonds. The lack of structural diversity in the glycine systems compared to that in the serine systems can partially be attributed to glycine's lack of a polar side chain. The hydroxymethyl side chain of serine gives the water molecules in the system an extra functional group to make hydrogen bonds, allowing for more intricate and diverse structures to form. Also, the $Gly(H_2O)_5$ system was the only glycine−water system where our global minimum structure was not in agreement with the one presented by Bachrach et al.[27] While the configurational sampling done by Bachrach et al. was adequate for glycine with one to four waters, it failed to find the lowest $Gly(H_2O)_5$ conformer because it did not take into account the impact of the amine nitrogen to form weak bonds with the water molecules. Obtaining accurate energies for clusters is difficult, and for water clusters alone, it generally requires high-level methods such as MP2 along with CCSD(T) corrections or CCSD(T)-level energy calculations.[73,90−97]

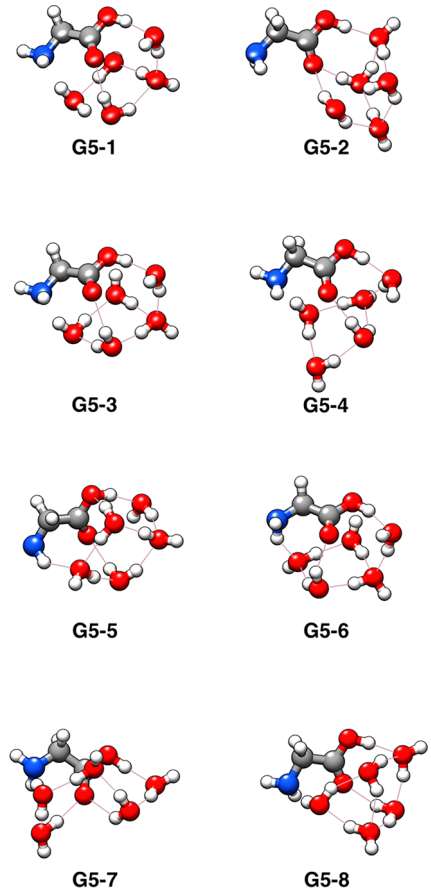

Figure 11. $Gly(H_2O)_5$ clusters within 2 kcal mol^{-1} of the ΔG°_{298} DLPNO-CCSD(T)/CBS//M08-HX/MG3S global minimum, G5-1. G5-3 is the ΔE_{el} DLPNO-CCSD(T) global minimum energy structure, G5-1 is the ΔG°_{298} M08-HX energy global minimum structure, and G5-8 is the ΔE_{el}M08-HX global minimum energy structure.

Thermodynamics of the Hydration of Glycine and Serine. We now explore the thermodynamics of the hydration of glycine and serine using the sequential hydration energies. Table 2 lists the numerical values for hydration, where each reaction involves the addition of n water molecules at temperatures of 216.65, 273.15, and 298.15 K and a pressure of 1 atm, while Figure 13 presents it sequentially. The absolute reaction energies are included in the Supporting Information. These temperatures correlate to tropospheric temperatures, with 216.65 K being the temperature at the top and 298.15 K being the temperature at the bottom of the troposphere. In the case of both the serine and glycine systems, the free energies will always be more negative at cooler temperatures, a consequence of the absolute value of $T\Delta S$ for the formation of a cluster from its constituent monomers. Note that even though these reactions are more energetically favorable to occur at cooler temperatures, the concentration of free water molecules is 3 orders of magnitude less at lower temperatures (and therefore at higher elevations).

https://doi.org/10.1021/acs.jpca.1c05466
J. Phys. Chem. A 2021, 125, 8454−8467

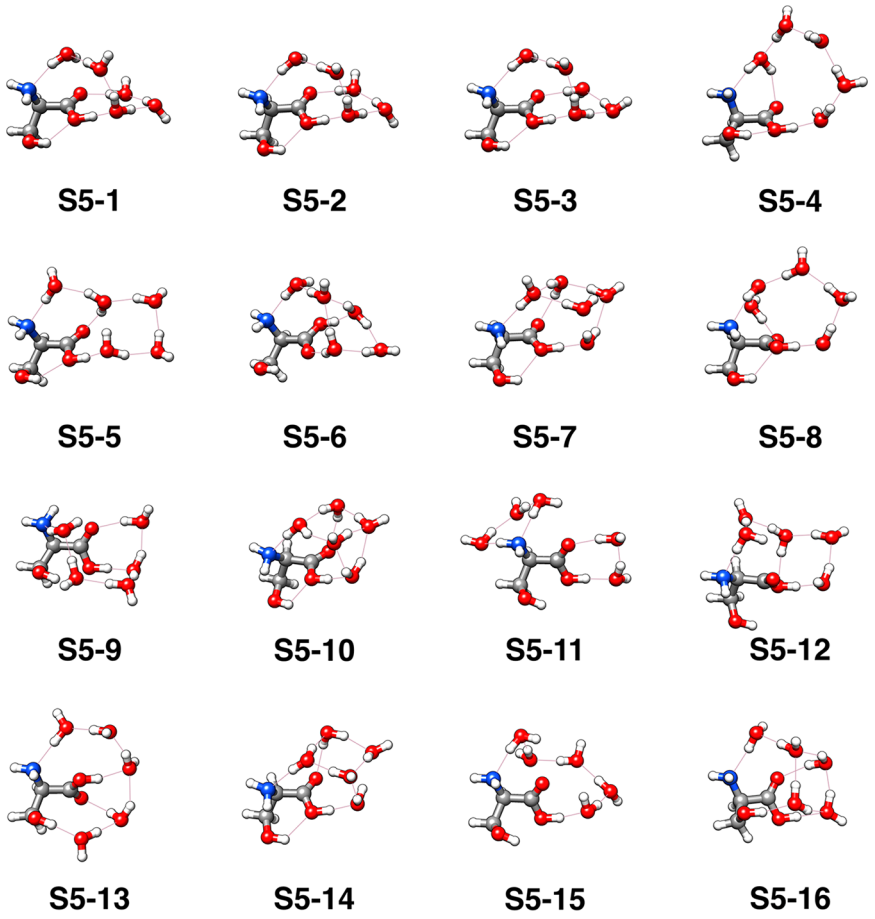

Figure 12. $Ser(H_2O)_5$ clusters within 2 kcal mol^{-1} of the $\Delta G°_{298}$ DLPNO-CCSD(T)/CBS//M08-HX/MG3S global minimum, S5-1. S5-16 is the ΔE_{el} DLPNO-CCSD(T) and ΔE_{el} and $\Delta G°_{298}$M08-HX global minimum structure.

Table 2. Relative Minimum Electronic Changes (ΔE_{el}) and Global Minimum Gibbs Free Energy Changes Associated with the Hydration ($\Delta G°_T$, standard state of 1 atm) of Glycine and Serine[a] by up to Five Water Molecules in the Gas Phase under 1 atm Pressure at Temperatures of 216.65, 273.15, and 298.15 K, Computed at the DLPNO-CCSD(T)/CBS//M08HX/MG3S Level of Theory

cluster	ΔE_{el}	$\Delta G°_{216}$	$\Delta G°_{273}$	$\Delta G°_{298}$
$Gly + H_2O \rightleftharpoons Gly(H_2O)_1$	−9.82	−1.29	0.48	1.25
$Gly + 2H_2O \rightleftharpoons Gly(H_2O)_2$	−20.56	−4.23	−0.86	0.63
$Gly + 3H_2O \rightleftharpoons Gly(H_2O)_3$	−28.76	−4.56	0.42	2.62
$Gly + 4H_2O \rightleftharpoons Gly(H_2O)_4$	−37.92	−5.06	1.73	4.72
$Gly + 5H_2O \rightleftharpoons Gly(H_2O)_5$	−47.66	−3.72	5.36	9.37
$Ser + H_2O \rightleftharpoons Ser(H_2O)_1$	−11.05	−2.78	−1.04	−0.28
$Ser + 2H_2O \rightleftharpoons Ser(H_2O)_2$	−18.45	−3.28	−0.06	1.35
$Ser + 3H_2O \rightleftharpoons Ser(H_2O)_3$	−29.36	−3.53	1.89	4.27
$Ser + 4H_2O \rightleftharpoons Ser(H_2O)_4$	−37.43	−3.77	3.22	6.30
$Ser + 5H_2O \rightleftharpoons Ser(H_2O)_5$	−45.00	−4.82	3.83	7.64

[a]Equation 1.

When performing calculations on clusters where hydrogen bonding plays a key role, it is crucial to keep in mind the importance of scaling harmonic frequencies or calculating anharmonic frequencies.[98−100] In previous research, we have used Truhlar's M08-HX/MG3S scaling factor (0.973) and applied it to the thermodynamics of formation for our lowest

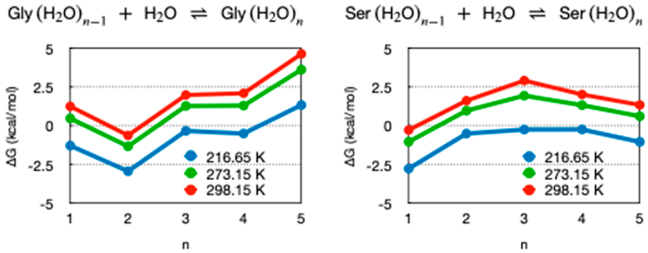

Figure 13. Gibbs free energies ($\Delta G°$) of the sequential hydration of glycine and serine (eq 2) as a function of the number of water molecules computed at the DLPNO-CCSD(T)/CBS//M08-HX/MG3S level of theory.

Gibbs free energy clusters and compared the resulting data to unscaled data.[74,101] Our group found the changes in the thermodynamic corrections used to compute the Gibbs free energy of formation to be negligible (about 0.19 kcal mol^{-1}), and this conclusion is supported by similar studies.[98,102,103] We also checked the effects of applying the quasiharmonic approximation, which applies scaling factors to low-frequency vibrational modes in the partition function,[104] and found no significant effect.[74]

Using the values presented in Table 2 and Figure 13, we find that in the cases of n = 1 and 5 the hydrated serine clusters have lower sequential $\Delta G°$ values and are more likely to form at all temperatures, given an equal concentration of glycine and serine. In all other cases, it is the hydrated glycine clusters that have the lower sequential $\Delta G°$ energies and therefore higher

https://doi.org/10.1021/acs.jpca.1c05466
J. Phys. Chem. A 2021, 125, 8454−8467

Table 3. Equilibrium Concentrations of $Gly(H_2O)_{n=0-5}$ and $Ser(H_2O)_{n=0-5}$ Computed Using a Starting Amino Acid Concentration of 1×10^6 Molecules per cm^3 and Water Concentrations of 9.89×10^{14} (at 217 K) to 7.70×10^{17} (at 298 K) Molecules per cm^3 for 100% Relative Humidity (RH) at Three Different Temperatures[106]

cluster	216.65 K	273.15 K	298.15 K
Gly	9.9×10^5	9.9×10^5	9.9×10^5
$Gly(H_2O)$	5.8×10^2	2.5×10^3	3.8×10^3
$Gly(H_2O)_2$	1.6×10^1	1.7×10^2	3.4×10^2
$Gly(H_2O)_3$	9.9×10^{-4}	9.7×10^{-2}	3.7×10^{-1}
$Gly(H_2O)_4$	9.4×10^{-8}	5.2×10^{-5}	3.3×10^{-4}
$Gly(H_2O)_5$	1.2×10^{-13}	3.8×10^{-10}	4.0×10^{-9}
Ser	9.8×10^5	9.6×10^5	9.5×10^5
$Ser(H_2O)$	1.8×10^4	3.9×10^4	4.7×10^4
$Ser(H_2O)_2$	1.7×10^0	3.8×10^1	9.6×10^1
$Ser(H_2O)_3$	8.9×10^{-5}	6.3×10^{-3}	2.2×10^{-2}
$Ser(H_2O)_4$	4.6×10^{-9}	3.2×10^{-6}	2.2×10^{-5}
$Ser(H_2O)_5$	1.5×10^{-12}	6.2×10^{-9}	7.2×10^{-8}

Table 4. Equilibrium Concentrations of $Gly(H_2O)_{n=0-5}$ and $Ser(H_2O)_{n=0-5}$ Computed Using a Starting Amino Acid Concentration of 1×10^8 Molecules per cm^3 and Water Concentrations Ranging from 9.89×10^{14} (at 217 K) to 7.70×10^{17} (at 298 K) Molecules per cm^3 for 100% Relative Humidity (RH) at Three Different Temperatures

cluster	216.65 K	273.15 K	298.15 K
Gly	9.9×10^7	9.9×10^7	9.9×10^7
$Gly(H_2O)$	5.8×10^4	2.5×10^5	3.8×10^5
$Gly(H_2O)_2$	1.6×10^3	1.7×10^4	3.4×10^4
$Gly(H_2O)_3$	9.9×10^{-2}	9.7×10^0	3.7×10^1
$Gly(H_2O)_4$	9.4×10^{-6}	5.2×10^{-3}	3.3×10^{-2}
$Gly(H_2O)_5$	1.2×10^{-11}	3.8×10^{-8}	4.0×10^{-7}
Ser	9.8×10^7	9.6×10^7	9.5×10^7
$Ser(H_2O)$	1.8×10^6	3.9×10^6	4.7×10^6
$Ser(H_2O)_2$	1.7×10^2	3.8×10^3	9.6×10^3
$Ser(H_2O)_3$	8.9×10^{-3}	6.3×10^{-1}	2.2×10^0
$Ser(H_2O)_4$	4.6×10^{-7}	3.2×10^{-4}	2.2×10^{-3}
$Ser(H_2O)_5$	1.5×10^{-10}	6.2×10^{-7}	7.2×10^{-6}

atmospheric concentrations when compared to the serine clusters with the same number of waters.

For each amino acid, the equilibrium concentrations were computed by solving the system of coupled stepwise hydration equations.[75] To compare the two on even footing, we chose initial amino acid concentrations of 1×10^6 and 1×10^8 molecules per cm^3 as well as their experimentally measured atmospheric concentrations: 2.43×10^9 molecules per cm^3 for glycine and 3.31×10^8 molecules per cm^3 for serine.[105] Table 3 lists the equilibrium concentrations for a system consisting of just each amino acid and water. At all temperatures, most of the amino acids exist as the monomer, with concentrations of around 10^6 cm^{-3}, while Tables 3 and 4 show the equilibrium concentrations when the initial amino acid concentration was 1×10^8 cm^{-3} along with the experimental values, respectively. For the systems that are hydrated, the glycine concentrations are larger at $n = 2-4$ while the serine concentrations are larger at $n = 1, 5$. This is to be expected because it follows the same trend of the Gibbs free energy changes of eq 2. This pattern of hydration is kept consistent even in Table 5, where glycine has a higher initial concentration than serine. The relative serine–water concentrations remain higher at $n = 1, 5$.

Table 5. Equilibrium Concentrations of $Gly(H_2O)_{n=0-5}$ and $Ser(H_2O)_{n=0-5}$ Computed Using a Starting Amino Acid Concentration of 2.43×10^9 Molecules per cm^3 for Glycine, 3.31×10^8 Molecules per cm^3 for Serine, and Water Concentrations Ranging from 9.89×10^{14} (at 217 K) to 7.70×10^{17} (at 298 K) Molecules per cm^3 for 100% Relative Humidity (RH) at Three Different Temperatures[a]

cluster	216.65 K	273.15 K	298.15 K
Gly	2.4×10^9	2.4×10^9	2.4×10^9
$Gly(H_2O)$	1.4×10^6	6.0×10^6	9.1×10^6
$Gly(H_2O)_2$	3.8×10^4	4.2×10^5	8.2×10^5
$Gly(H_2O)_3$	2.4×10^0	2.3×10^2	8.9×10^2
$Gly(H_2O)_4$	2.3×10^{-4}	1.3×10^{-1}	8.0×10^{-1}
$Gly(H_2O)_5$	3.0×10^{-10}	9.3×10^{-7}	9.8×10^{-6}
Ser	3.3×10^8	3.2×10^8	3.2×10^8
$Ser(H_2O)$	6.0×10^6	1.3×10^7	1.6×10^7
$Ser(H_2O)_2$	5.7×10^2	1.3×10^4	3.2×10^4
$Ser(H_2O)_3$	3.0×10^{-2}	2.1×10^0	7.1×10^0
$Ser(H_2O)_4$	1.5×10^{-6}	1.1×10^{-3}	7.3×10^{-3}
$Ser(H_2O)_5$	5.0×10^{-10}	2.1×10^{-6}	2.3×10^{-5}

[a]The glycine and serine concentrations were taken from experimental values in the literature.[105]

Unlike the sulfuric acid-based CCN that were studied prior to our research, glycine and serine tend to remain as a monomer or hydrated with one water at all temperatures. However, when using the experimental concentrations of glycine and serine found by Ren et al., we still find appreciable amounts of hydrated serine and glycine when $n = 1$ to 2. The observation that the amino acids remain primarily as monomers is consistent with other clusters involving the hydration of organic acids without sulfuric acid. Atmospheric sulfuric acid tends to exist in a hydrated form with substantial concentrations of one to four waters, depending on the temperature at 100% relative humidity.[102] Temelso et al. also found relative concentrations of the hydrated sulfuric acid dimer compared to the sulfuric acid monomer and inferred that, except at the coldest temperatures, the concentrations of the hydrated dimer will be unsubstantial.[103] Ions have a more dramatic effect on predicted equilibrium concentrations. Husar et al. calculated atmospheric concentrations of the hydrated bisulfate ion and predicted that it exists primarily in clusters containing two to three waters, with substantial numbers of clusters with four to five waters at 100% relative humidity.[107] Morrell et al. studied the hydration of the ammonium ion and predicted that it exists mostly in clusters with four to five waters, with notable concentrations of clusters with three and six waters.[108] Bustos et al. investigated the hydration concentrations of clusters consisting of sulfuric acid, methylamine, and zero to six waters.[109] The equilibrium prediction is that at all temperatures and at all relative levels of humidity, sulfuric acid and methylamine overwhelmingly exist in clusters hydrated with two waters.[109] Kildgaard et al. have investigated the relative concentrations of the hydrated clusters for three different organic acids (pinic acid, 3-methyl-1,2,3-butanetricarboxylic acid, and 2-oxohexanediperoxy acid) with 1–10 waters, and their results inferred that all three organic acids overwhelmingly exist in their monomer form in the atmosphere.[110] Clusters of other sulfur compounds, such as OCS and CS_2, along with HO_2, have been predicted to form a small number of hydrated structures in the atmosphere.[111−113] Elm has shown that sulfuric acid is a much better nucleator than methanesulfonic acid.[114,115] Ge et al. have found relative concentrations for clusters of serine and sulfuric

https://doi.org/10.1021/acs.jpca.1c05466
J. Phys. Chem. A 2021, 125, 8454−8467

Table 6. Electronic Energy Changes Associated with the Formation of Hydrated Amino Glycine and Serine Clusters from Infinitely Separated Monomers Calculated at the M08-HX/MG3S DFT Level and DLPNO-CCSD(T)/cc-pVnZ//M08-HX/MG3S Level with (n = D, T, Q) and the Complete Basis Set (CBS) Limit[a]

		DLPNO-CCSD(T)			
	M08-HX/MG3S	cc-pVDZ	cc-pVTZ	cc-pVQZ	CBS
$Gly(H_2O)$	−11.6	−13.3	−11.3	−10.6	−9.8
$Gly(H_2O)_2$	−23.1	−27.1	−23.3	−21.8	−20.6
$Gly(H_2O)_3$	−32.0	−37.8	−32.7	−30.6	−28.8
$Gly(H_2O)_4$	−42.9	−51.5	−44.0	−40.8	−37.9
$Gly(H_2O)_5$	−56.1	−70.4	−58.5	−53.0	−47.6
$Ser(H_2O)$	−12.1	−13.3	−11.9	−11.3	−10.6
$Ser(H_2O)_2$	−21.5	−25.8	−22.2	−20.8	−19.5
$Ser(H_2O)_3$	−33.5	−43.3	−35.6	−32.3	−29.4
$Ser(H_2O)_4$	−42.4	−54.4	−45.2	−41.0	−37.1
$Ser(H_2O)_5$	−57.7	−71.5	−58.8	−53.6	−48.8

[a]All units are in kcal mol^{-1}.

acid with zero to three waters, and while our data indicates that serine remains as a monomer or hydrated with one water in the atmosphere, Ge found that when serine is in a cluster with sulfuric acid, it should exist primarily as hydrated clusters with one to two water molecules.[3] Overall, these results lead to the prediction that neutral amino acids by themselves will not be effective at forming prenucleation complexes in the troposphere. Amino acids with charged side chains should be investigated.

Effects of Complete Basis Set Extrapolations. At this point, we discuss the effects of using DLPNO-CCSD(T) electronic energies at the complete basis set limit. In most studies concerning the PES and configurational energies of certain gas-phase molecular clusters, the absolute energies are of main interest so that a detailed energy ordering of different conformers and configurations can be constructed. In contrast, atmospheric aerosol studies focus on the energies associated with the formation of gas-phase clusters from separated monomers so that clustering processes can be studied. In both cases, it is expedient to use DFT geometries and vibrational energies along with higher-level electronic energies such as DLPNO-CCSD(T), and often a triple-ζ basis set is employed. We have found in this work that while larger basis sets may lower the absolute energies of the clusters and monomers, they also make the formation energies more positive, with the most positive value being the CBS extrapolated energy. This means that at any basis set other than the CBS limit, the cluster's formation energy is erroneously low (more negative) and thus the concentration of said cluster is overestimated in subsequent calculations. This is shown in Table 6 where the electronic energies associated with eq 1 in the methodologies section are shown for the global minima of $Gly(H_2O)_n$ and $Ser(H_2O)_n$ (n = 1−5) in units of kcal mol^{-1}. The raw energies used to compute these reaction energies are listed in the spreadsheet raw-energies.xlsx in the Supporting Information.

For all systems listed, Table 6 shows that the DLPNO-CCSD(T) reaction energies are more negative than the DFT energies at the double-ζ basis set and are quite close to the DFT values at the triple-ζ basis set. This means that using just DLPNO-CCSD(T)/cc-pVTZ numbers will at best reproduce the DFT energies, defeating the purpose of the high-level quantum chemistry correction. The quadruple-ζ basis sets are more positive, and this trend continues to the complete basis set limit. This overestimation of up to a few kcal mol^{-1} is larger than the other contributions to the free-energy change of the reactions, and 1.4 kcal mol^{-1} in the free-energy change corresponds to 1 order of magnitude change in the equilibrium constant at 298 K.

CONCLUSIONS

We have thoroughly explored the configuration space of $Gly(H_2O)_{n=1-5}$ and $Ser(H_2O)_{n=1-5}$ within 2 kcal mol^{-1} of the global ΔG°_{298} minimum. We predicted that the equilibrium concentration of $Ser(H_2O)_{1,5}$ will be higher than that of $Gly(H_2O)_{1,5}$, while $Gly(H_2O)_{2-4}$ will have higher concentrations than $Ser(H_2O)_{2-4}$. When the serine systems are more favorable to form, they have more hydrogen bonds than the glycine systems; however, when the glycine systems are more favorable, it is due to particularly stable water clusters with two water molecules replaced by the carboxyl group of the amino acid. This shows that in the gas-phase molecular size regime, having a hydrophilic functional group does not always mean stronger binding to water molecules. In fact, a large enough hydrophilic functional group can block water molecules because intramolecular hydrogen bonds compete with intermolecular hydrogen bonds. Also, in the case of the serine−water clusters, it is vital that a thorough investigation into the configurational space is carried out. Previous research into the $Ser(H_2O)_n$ system has missed many of the geometries we present herein because of a lack of proper configurational sampling. Serine and amino acids in general have an abundance of possible hydrogen bonding sites such that adequate configurational sampling is critical.

Calculating accurate Gibbs free energy values for the formation of clusters from their monomer constituents requires CCSD(T)/CBS-level calculations. Extrapolation to the complete basis set limit is essential to obtaining accurate ΔG values. DFT and CCSD(T)/cc-pVTZ energies are too negative relative to CCSD(T)/CBS values, thereby overestimating the degree of cluster formation. This will lead to large errors in understanding nucleation.

Because both glycine and serine remain primarily in their monomer forms in the atmosphere, they do not reach the critical size needed to become a CCN, which is about 1 nm. There is still an appreciable amount of $Ser(H_2O)$ system in the atmosphere, but this system also does not reach the critical size of 1 nm, and only reaches a radius between 0.6−0.7 nm and because of this, we conclude that most neutral charged amino acids by themselves will not lead to aerosol nucleation. While the hydrated monomers of serine and glycine do not reach a critical size, the work done by Ge et al. shows that serine along with other common atmospheric molecules, such as sulfuric acid, do tend to hydrate with waters and might reach sizes that

https://doi.org/10.1021/acs.jpca.1c05466
J. Phys. Chem. A 2021, 125, 8454−8467

could qualify them as CCN.[3] In addition, because ions have greater hydration, charged amino acids should be investigated as potential CCN. Our group has begun looking into the hydration reactions of larger systems composed of amino acids and other species that have shown potential as CCN.

■ ASSOCIATED CONTENT

Supporting Information

The Supporting Information is available free of charge at https://pubs.acs.org/doi/10.1021/acs.jpca.1c05466.

M08-HX/MG3S coordinate files, electronic energies, G correction values, DLPNO-CCSD(T) electronic energies with the cc-pVnZ basis sets (n = D,T,Q), and CBS extrapolation formulas (ZIP)

■ AUTHOR INFORMATION

Corresponding Author

George C. Shields − *Department of Chemistry, Furman University, Greenville, South Carolina 29613, United States;* orcid.org/0000-0003-1287-8585; Email: george.shields@furman.edu

Authors

Benjamin T. Ball − *Department of Chemistry, Furman University, Greenville, South Carolina 29613, United States*

Sara Vanovac − *Department of Chemistry, Furman University, Greenville, South Carolina 29613, United States*

Tuguldur T. Odbadrakh − *Department of Chemistry, Furman University, Greenville, South Carolina 29613, United States*

Complete contact information is available at: https://pubs.acs.org/10.1021/acs.jpca.1c05466

Notes

The authors declare no competing financial interest.

■ ACKNOWLEDGMENTS

Funding for this work was provided by grants CHE-1229354, CHE 1662030, CHE-1903871, and CHE-2018427 from the National Science Foundation (GCS). High-performance computing resources were provided by the Research Corporation for Science Advancement (27446) and the MERCURY Consortium (www.mercuryconsortium.org).[116] Molecular graphics and analyses were performed with UCSF Chimera, developed by the Resource for Biocomputing, Visualization, and Informatics at the University of California, San Francisco, with support from NIH P41-GM103311.

■ REFERENCES

(1) Novakov, T.; Penner, J. E. Large contribution of organic aerosols to cloud-condensation-nuclei concentrations. *Nature* **1993**, *365*, 823−826.

(2) Elm, J.; Fard, M.; Bilde, M.; Mikkelsen, K. V. Interaction of glycine with common atmospheric nucleation precursors. *J. Phys. Chem. A* **2013**, *117* (48), 12990−7.

(3) Ge, P.; Luo, G.; Luo, Y.; Huang, W.; Xie, H.; Chen, J.; Qu, J. Molecular understanding of the interaction of amino acids with sulfuric acid in the presence of water and the atmospheric implication. *Chemosphere* **2018**, *210*, 215−223.

(4) Griffith, E. C.; Vaida, V. In situ observation of peptide bond formation at the water-air interface. *Proc. Natl. Acad. Sci. U. S. A.* **2012**, *109* (39), 15697−701.

(5) Kristensson, A.; Rosenorn, T.; Bilde, M. Cloud droplet activation of amino acid aerosol particles. *J. Phys. Chem. A* **2010**, *114* (1), 379−86.

(6) Liu, Y.; Liu, Y.-R.; Feng, Y.-J.; Huang, T.; Jiang, S.; Wang, Z.-H.; Cao, H.; Huang, W. Valine involved sulfuric acid-dimethylamine ternary homogeneous nucleation and its atmospheric implications. *Atmos. Environ.* **2021**, *254*, 118373.

(7) Gale, A. G.; Odbadrakh, T. T.; Ball, B. T.; Shields, G. C. Water-Mediated Peptide Bond Formation in the Gas Phase: A Model Prebiotic Reaction. *J. Phys. Chem. A* **2020**, *124* (20), 4150−4159.

(8) Gale, A. G.; Odbadrakh, T. T.; Shields, G. C., Catalytic activity of water molecules in gas-phase glycine dimerization. *Int. J. Quantum Chem.* **2020**, *120* (20), DOI: 10.1002/qua.26469.

(9) Dobson, C. M.; Ellison, G. B.; Tuck, A. F.; Vaida, V. Atmospheric aerosols as prebiotic chemical reactors. *Proc. Natl. Acad. Sci. U. S. A.* **2000**, *97* (22), 11864−8.

(10) Frenkel-Pinter, M.; Samanta, M.; Ashkenasy, G.; Leman, L. J. Prebiotic Peptides: Molecular Hubs in the Origin of Life. *Chem. Rev.* **2020**, *120* (11), 4707−4765.

(11) Ruiz-Mirazo, K.; Briones, C.; Escosura, d. l. Prebiotic systems chemistry: new perspectives for the origins of life. *Chem. Rev.* **2014**, *114*, 285−366.

(12) Leonardi, A.; Ricker, H. M.; Gale, A. G.; Ball, B. T.; Odbadrakh, T. T.; Shields, G. C.; Navea, J. G., Particle formation and surface processes on atmospheric aerosols: A review of applied quantum chemical calculations. *Int. J. Quantum Chem.* **2020**, *120*, DOI: 10.1002/qua.26350.

(13) Miller, S. L. A production of amino acids under possible primitive earth conditions. *Science* **1953**, *117* (3046), 528−9.

(14) Parker, E. T.; Zhou, M.; Burton, A. S.; Glavin, D. P.; Dworking, J. P.; Krishnamurthy, R.; Fernandez, F. M.; Bada, J. L. A plausible simultaneous synthesis of amino acids and simple peptides on the primordial Earth. *Angew. Chem., Int. Ed.* **2014**, *53* (31), 8132−8136.

(15) Bernstein, M. P.; Dworkin, J. P.; Sandford, S. A.; Cooper, G. W.; Allamandola, L. J. Racemic amino acids from the ultraviolet photolysis of interstellar ice analogues. *Nature* **2002**, *416* (6879), 401−3.

(16) Kvenvolden, K.; Lawless, J.; Pering, K.; Peterson, E.; Flores, J.; Ponnamperuma, C.; Kaplan, I. R.; Moore, C. Evidence for extraterrestrial amino-acids and hydrocarbons in the Murchison meteorite. *Nature* **1970**, *228* (5275), 923−6.

(17) Pizzarello, S.; Shock, E. The organic composition of carbonaceous meteorites: the evolutionary story ahead of biochemistry. *Cold Spring Harbor Perspect. Biol.* **2010**, *2* (3), No. a002105.

(18) Helin, A.; Sietiö, O.-M.; Heinonsalo, J.; Bäck, J.; Riekkola, M.-L.; Parshintsev, J. Characterization of free amino acids, bacteria and fungi in size-segregated atmospheric aerosols in boreal forest: seasonal patterns, abundances and size distributions. *Atmos. Chem. Phys.* **2017**, *17* (21), 13089−13101.

(19) Mandalakis, M.; Apostolaki, M.; Stephanou, E. G. Trace analysis of free and combined amino acids in atmospheric aerosols by gas chromatography-mass spectrometry. *Journal of Chromatography A* **2010**, *1217* (1), 143−50.

(20) Matsumoto, K.; Uematsu, M. Free amino acids in marine aerosols over the western North Pacific Ocean. *Atmos. Environ.* **2005**, *39* (11), 2163−2170.

(21) Ge, X.; Wexler, A. S.; Clegg, S. L. Atmospheric amines - Part I. A review. *Atmos. Environ.* **2011**, *45* (3), 524−546.

(22) Ge, X.; Wexler, A. S.; Clegg, S. L. Atmospheric amines - Part II. Thermodynamic properties and gas/particle partitioning. *Atmos. Environ.* **2011**, *45* (3), 561−577.

(23) Hinds, W. C. *Aerosol Technology: Properties, Behavior, and Measurement of Airborne Particles*, 2nd ed.; 1999.

(24) Ahn, D. S.; Kang, A. R.; Lee, S.; Kim, B.; Kyu Kim, S.; Neuhauser, D. On the stability of glycine-water clusters with excess electron: implications for photoelectron spectroscopy. *J. Chem. Phys.* **2005**, *122* (8), 084310.

(25) Aikens, C. M.; Gordon, M. S. Incremental solvation of nonionized and zwitterionic glycine. *J. Am. Chem. Soc.* **2006**, *128*, 12835−12850.
(26) Alonso, J. L.; Cocinero, E. J.; Lesarri, A.; Sanz, M. E.; López, J. C. The glycine-water complex. *Angew. Chem.* **2006**, *118*, 3551−3554.
(27) Bachrach, S. M. Microsolvation of glycine: a DFT study. *J. Phys. Chem. A* **2008**, *112*, 3722−3730.
(28) Balabin, R. M. The first step in glycine solvation: the glycine-water complex. *J. Phys. Chem. B* **2010**, *114*, 15075−15078.
(29) Di Gioacchino, M.; Ricci, M. A.; Imberti, S.; Holzmann, N.; Brumni, F. Hydration and aggregation of a simple amino acid: The case of glycine. *J. Mol. Liq.* **2020**, *301*, 112407.
(30) Espinoza, C.; Szczepanski, J.; Vala, M.; Polfer, N. C. Glycine and its hydrated complexes: a matrix isolation infrared study. *J. Phys. Chem. A* **2010**, *114*, 5919−27.
(31) Kishimoto, N. An automated and efficient conformational search of glycine and a glycine-water heterodimer both in vacuum and in aqueous solution. *Chem. Phys. Lett.* **2017**, *667*, 172−179.
(32) Kocs, L.; Najbauer, E. E.; Bazso, G.; Magyarfalvi, G.; Tarczay, G. Near-infrared laser-induced structural changes of glycine-water complexes in an Ar matrix. *J. Phys. Chem. A* **2015**, *119*, 2429−2437.
(33) Perez de Tudela, R.; Marx, D. Water-Induced Zwitterionization of Glycine: Stabilization Mechanism and Spectral Signatures. *J. Phys. Chem. Lett.* **2016**, *7* (24), 5137−5142.
(34) Ramaekers, R.; Pajak, J.; Lambie, B.; Maes, G. Neutral and zwitterionic glycine.H(2)O complexes: A theoretical and matrix-isolation Fourier transform infrared study. *J. Chem. Phys.* **2004**, *120*, 4182−4193.
(35) Sun, J.; Xu, Z.; Liu, X. Structures and stabilities of glycine and water complexes. *Chem. Phys.* **2020**, *528*, 110528.
(36) Tripathi, R.; Duran Caballero, L.; Perez de Tudela, R.; Holzl, C.; Marx, D. Unveiling Zwitterionization of Glycine in the Microhydration Limit. *ACS Omega* **2021**, *6* (19), 12676−12683.
(37) Yanase, S.; Musashi, M.; Oi, T. Nitrogen isotopic reduced partition function ratios of glycine and serine in water. *J. Phys. Chem. A* **2020**, *124*, 5212−5229.
(38) Blanco, S.; Sanz, M. E.; Lopez, J. C.; Alonso, J. L. Revealing the multiple structures of serine. *Proc. Natl. Acad. Sci. U. S. A.* **2007**, *104*, 20183−20188.
(39) Chopra, G.; Chopra, N.; Kaur, D. Quantum chemical study of hydrogen-bonded complexes of serine with water and H2O2. *J. Chem. Sci.* **2018**, *130*, 112.
(40) He, K.; Allen, W. D. Conformers of gaseous serine. *J. Chem. Theory Comput.* **2016**, *12*, 3571−3582.
(41) Jeon, I.-S.; Ahn, D.-S.; Park, S.-W.; Lee, S.; Kim, B. Structures and isomerization of neutral and zwitterion serine-water clusters: Computational study. *Int. J. Quantum Chem.* **2005**, *101* (1), 55−66.
(42) Lambie, B.; Ramaekers, R.; Maes, G. Conformational behavior of serine: An experimental matrix-isolation FT-IR and theoretical DFT(B3LYP)/6-31++G** study. *J. Phys. Chem. A* **2004**, *108*, 10426−10433.
(43) Li, L.; Zhang, R.; Ma, X.; Wei, Y.; Zhao, X.; Zhang, R.; Xu, F.; Li, Y.; Huo, X.; Zhang, Q. Gas-phase and aqueous-surface reaction mechanism of Criegee radicals with serine and nucleation of products: A theoretical study. *Chemosphere* **2021**, *280*, 130709.
(44) Miao, R.; Jin, C.; Yang, G.; Hong, J.; Zhao, C.; Zhu, L. Comprehensive density functional theory study on serine and related ions in gas phase: conformations, gas phase basicities, and acidities. *J. Phys. Chem. A* **2005**, *109*, 2340−2349.
(45) Najbauer, E. E.; Bazso, G.; Apostolo, R.; Fausto, R.; Biczysko, M.; Barone, V.; Tarczay, G. Identification of serine conformers by matrix-isolation IR spectroscopy aided by near-infrared laser-induced conformational change, 2D correlation analysis, and quantum mechanical anharmonic computations. *J. Phys. Chem. B* **2015**, *119*, 10496−10510.
(46) Ramırez, F.J.; Tunon, I.; Silla, E. Amino acid chemistry in solution: structural properties and vibrational dynamics of serine using density functional theory and a continuum solvent model. *Chem. Phys.* **2004**, *303*, 85−96.
(47) Zhu, P.; Yang, G.; Poopari, M. R.; Bie, Z.; Xu, Y. Conformations of serine in aqueous solutions as revealed by vibrational circular dichroism. *ChemPhysChem* **2012**, *13*, 1272−1281.
(48) Bannwarth, C.; Ehlert, S.; Grimme, S. GFN2-xTB-An accurate and broadly parametrized self- consistent tight-binding quantum chemical method with multipole electrostatics and density-dependent dispersion contributions. *J. Chem. Theory Comput.* **2019**, *15*, 1652−1672.
(49) Grimme, S. Exploration of Chemical Compound, Conformer, and Reaction Space with Meta-Dynamics Simulations Based on Tight-Binding Quantum Chemical Calculations. *J. Chem. Theory Comput.* **2019**, *15* (5), 2847−2862.
(50) Dieterich, J. M.; Hartke, B. OGOLEM: Global cluster structure optimization for arbitrary mixtures of flexible molecules. A multi-scaling, object-oriented approach. *Mol. Phys.* **2010**, *108*, 279−291.
(51) Forck, R. M.; Dieterich, J. M.; Pradzynski, C. C.; Huchting, A. L.; Mata, R. A.; Zeuch, T. Structural diversity in sodium doped water trimers. *Phys. Chem. Chem. Phys.* **2012**, *14*, 9054−9057.
(52) Dieterich, J. M.; Hartke, B. Empirical review of standard benchmark functions using evolutionary global optimization. *Appl. Math.* **2012**, *03*, 1552.
(53) Dieterich, J. M.; Hartke, B. Composition-induced structural transitions in mixed Lennard-Jones clusters: global reparametrization and optimization. *J. Comput. Chem.* **2011**, *32*, 1377−1385.
(54) Witt, C.; Dieterich, J. M.; Hartke, B. Cluster structures influenced by interaction with a surface. *Phys. Chem. Chem. Phys.* **2018**, *20* (23), 15661−15670.
(55) Freibert, A.; Dieterich, J. M.; Hartke, B. Exploring self-organization of molecular tether molecules on a gold surface by global structure optimization. *J. Comput. Chem.* **2019**, *40* (22), 1978−1989.
(56) Carstensen, N. O.; Dieterich, J. M.; Hartke, B. Design of optimally switchable molecules by genetic algorithms. *Phys. Chem. Chem. Phys.* **2011**, *13*, 2903−2910.
(57) Hostas, J.; Rezac, J.; Hobza, P. On the performance of the semiempirical quantum mechanical PM6 and PM7 methods for noncovalent interactions. *Chem. Phys. Lett.* **2013**, *568*−*569*, 161−166.
(58) Stewart, J. J. P. *MOPAC2016, Stewart Computational Chemistry*; Colorado Springs, CO, 2016.
(59) Hostaš, J.; Rezáč, J.; Hobza, P. On the performance of the semiempirical quantum mechanical PM6 and PM7 methods for noncovalent interactions. *Chem. Phys. Lett.* **2013**, *568*−*569*, 161−166.
(60) Stewart, J. J. P. An investigation into the applicability of the semiempirical method PM7 for modeling the catalytic mechanism in the enzyme chymotrypsin. *J. Mol. Model.* **2017**, *23*, 154.
(61) Hourahine, B.; Aradi, B.; Blum, V.; Bonafe, F.; Buccheri, A.; Camacho, C.; Cevallos, C.; Deshaye, M. Y.; Dumitrica, T.; Dominguez, A.; et al. DFTB+, a software package for efficient approximate density functional theory based atomistic simulations. *J. Chem. Phys.* **2020**, *152*, 124101.
(62) Zhao, Y.; Truhlar, D. G. Exploring the limit of accuracy of the global hybrid meta density functional for main-group thermochemistry, kinetics, and noncovalent interactions. *J. Chem. Theory Comput.* **2008**, *4*, 1849−1868.
(63) Ditchfield, R.; Hehre, W. J.; Pople, J. A. Self-consistent molecular orbital methods. IX. Extended Gaussian-type basis for molecular-orbital studies of organic molecules. *J. Chem. Phys.* **1971**, *54*, 724.
(64) Ditchfield, R.; Hehre, W. J.; Pople, J. A. Self-Consistent Molecular-Orbital Methods. IX. An Extended Gaussian-Type Basis for Molecular-Orbital Studies of Organic Molecules. *J. Chem. Phys.* **1971**, *54* (2), 724−728.
(65) Frisch, M. J.; Pople, J. A.; Binkley, J. S. Self-consistent molecular orbital methods 25. Supplementary functions for Gaussian basis sets. *J. Chem. Phys.* **1984**, *80*, 3265−3269.
(66) Hehre, W. J.; Ditchfield, R.; Pople, J. A. Self-consistent molecular orbital methods. 12. Further extensions of Gaussian-type sets for use in molecular-orbital studies of organic molecules. *J. Chem. Phys.* **1972**, *56*, 2257−2261.

https://doi.org/10.1021/acs.jpca.1c05466
J. Phys. Chem. A 2021, 125, 8454−8467

(67) Krishnan, R.; Binkley, J. S.; Seeger, R.; Pople, J. A. Self-consistent molecular orbital methods. XX. A basis set for correlated wave functions. *J. Chem. Phys.* **1980**, *72*, 650−654.
(68) Frisch, M. J.; Trucks, G. W.; Schlegel, H. B.; Scuseria, G. E.; Robb, M. A.; Cheeseman, J. R.; Scalmani, G.; Barone, V.; Petersson, G. A.; Nakatsuji, H.; et al. *Gaussian 16, Rev. B.01*; Wallingford, CT, 2016.
(69) Irikura, K. K. *THERMO.PL*; NIST, 2002.
(70) Neese, F. The ORCA program system. *Wiley Interdiscip. Rev.: Comput. Mol. Sci.* **2012**, *2*, 73−78.
(71) Neese, F. Software update: the ORCA program system. *Wiley Interdiscip. Rev.: Comput. Mol. Sci.* **2018**, *8*, e1327.
(72) Helgaker, T.; Klopper, W.; Koch, H.; Noga, J. Basis-set convergence of correlated calculations on water. *J. Chem. Phys.* **1997**, *106*, 9639−9646.
(73) Temelso, B.; Shields, G. C. The Role of Anharmonicity in Hydrogen-Bonded Systems: The Case of Water Clusters. *J. Chem. Theory Comput.* **2011**, *7* (9), 2804−2817.
(74) Kurfman, L. A.; Odbadrakh, T. T.; Shields, G. C. Calculating Reliable Gibbs Free Energies for Formation of Gas-Phase Clusters that Are Critical for Atmospheric Chemistry: (H2SO4)3. *J. Phys. Chem. A* **2021**, *125* (15), 3169−3176.
(75) Odbadrakh, T. T.; Gale, A. G.; Ball, B. T.; Temelso, B.; Shields, G. C. Computation of atmospheric concentrations of molecular clusters from ab initio thermochemistry. *J. Visualized Exp.* **2020**, *158*, e60964.
(76) Schmitz, G.; Elm, J. Assessment of the DLPNO binding energies of strongly noncovalent bonded atmospheric molecular clusters. *ACS Omega* **2020**, *5* (13), 7601−7612.
(77) Elm, J.; Mikkelsen, K. V. Computational approaches for efficiently modelling of small atmospheric clusters. *Chem. Phys. Lett.* **2014**, *615*, 26−29.
(78) Elm, J.; Bilde, M.; Mikkelsen, K. V. Assessment of binding energies of atmospherically relevant clusters. *Phys. Chem. Chem. Phys.* **2013**, *15*, 16442−16445.
(79) Kurfman, L. A.; Odbadrakh, T. T.; Shields, G. C. Calculating Reliable Gibbs Free Energies for Formation of Gas-Phase Clusters that Are Critical for Atmospheric Chemistry: (H2SO4)3. *J. Phys. Chem. A* **2021**, *125* (15), 3169−3176.
(80) Hariharan, P. C.; Pople, J. A. The influence of polarization functions on molecular orbital hydrogenation energies. *Theoretica Chimica Acta* **1973**, *28*, 213−222.
(81) Hehre, W. J.; Ditchfield, R.; Pople, J. A. Self-consistent molecular orbital methods 12. Further extensions of Gaussian-type sets for use in molecular-orbital studies of organic molecules. *J. Chem. Phys.* **1972**, *56*, 2257−2261.
(82) Ditchfield, R.; Hehre, W. J.; Pople, J. A. Self-consistent molecular-orbital methods. IX. An extended Gaussian-type basis for molecular-orbital studies of organic molecules. *J. Chem. Phys.* **1971**, *54*, 724−728.
(83) Barone, V.; Biczysko, M.; Bloino, J.; Puzzarini, C. Characterization of the elusive conformers of glycine from state-of-the-art structural, thermodynamic, and spectroscopic computations: Theory complements experiment. *J. Chem. Theory Comput.* **2013**, *9* (3), 1533−47.
(84) Chang, X.; Chen, Z.; Su, P.; Wu, W. The C O rotation in the gaseous glycine. An energy decomposition analysis study. *Chem. Phys. Lett.* **2015**, *640*, 194−200.
(85) Liptak, M. D.; Shields, G. C. Comparison of density functional theory predictions of gas-phase deprotonation data. *Int. J. Quantum Chem.* **2005**, *105* (6), 580−587.
(86) Pickard, F. C.; Dunn, M. E.; Shields, G. C. Comparison of model chemistry and density functional theory thermochemical predictions with experiment for formation of ionic clusters of the ammonium cation complexed with water and ammonia; Atmospheric implications. *J. Phys. Chem. A* **2005**, *109* (22), 4905−4910.
(87) Pickard, F. C.; Griffith, D. R.; Ferrara, S. J.; Liptak, M. D.; Kirschner, K. N.; Shields, G. C. CCSD(T), W1, and other model chemistry predictions for gas-phase deprotonation reactions. *Int. J. Quantum Chem.* **2006**, *106* (15), 3122−3128.
(88) Pickard, F. C.; Pokon, E. K.; Liptak, M. D.; Shields, G. C. Comparison of CBS-QB3, CBS-APNO, G2, and G3 thermochemical predictions with experiment for formation of ionic clusters of hydronium and hydroxide ions complexed with water. *J. Chem. Phys.* **2005**, *122* (2), 024302.
(89) Shields, G. C.; Kirschner, K. N. The Limitations of Certain Density Functionals in Modeling Neutral Water Clusters. *Synth. React. Inorg., Met.-Org., Nano-Met. Chem.* **2008**, *38* (1), 32−39.
(90) Shields, R. M.; Temelso, B.; Archer, K. A.; Shields, G. C. Accurate predictions of water cluster formation, (H2O)n = 2−10. *J. Phys. Chem. A* **2010**, *114* (43), 11725−11737.
(91) Temelso, B.; Archer, K. A.; Shields, G. C. Benchmark Structures and Binding Energies of Small Water Clusters with Anharmonicity Corrections. *J. Phys. Chem. A* **2011**, *115* (43), 12034−12046.
(92) Dunn, M. E.; Pokon, E. K.; Shields, G. C. Thermodynamics of forming water clusters at various temperatures and pressures by Gaussian-2, Gaussian-3, Complete Basis Set-QB3, and Complete Basis Set-APNO model chemistries; Implications for atmospheric chemistry. *J. Am. Chem. Soc.* **2004**, *126* (8), 2647−2653.
(93) Dunn, M. E.; Pokon, E. K.; Shields, G. C. The ability of the Gaussian-2, Gaussian-3, Complete Basis Set-QB3, and Complete Basis Set-APNO model chemistries to model the geometries of small water clusters. *Int. J. Quantum Chem.* **2004**, *100* (6), 1065−1070.
(94) Pérez, C.; Muckle, M. T.; Zaleski, D. P.; Seifert, N. A.; Temelso, B.; Shields, G. C.; Kisiel, Z.; Pate, B. H. Structures of Cage, Prism, and Book Isomers of Water Hexamer from Broadband Rotational Spectroscopy. *Science* **2012**, *336* (6083), 897−901.
(95) Howard, J. C.; Gray, J. L.; Hardwick, A. J.; Nguyen, L. T.; Tschumper, G. S. Getting down to the Fundamentals of Hydrogen Bonding: Anharmonic Vibrational Frequencies of (HF)2 and (H2O)2 from Ab Initio Electronic Structure Computations. *J. Chem. Theory Comput.* **2014**, *10* (12), 5426−35.
(96) Temelso, B.; Renner, C. R.; Shields, G. C. Importance and Reliability of Small Basis Set CCSD(T) Corrections to MP2 Binding and Relative Energies of Water Clusters. *J. Chem. Theory Comput.* **2015**, *11* (4), 1439−1448.
(97) Temelso, B.; Klein, K. L.; Mabey, J. W.; Perez, C.; Pate, B. H.; Kisiel, Z.; Shields, G. C. Exploring the Rich Potential Energy Surface of (H2O)(11) and Its Physical Implications. *J. Chem. Theory Comput.* **2018**, *14* (2), 1141−1153.
(98) Dunn, M. E.; Evans, T. M.; Kirschner, K. N.; Shields, G. C. Prediction of accurate anharmonic experimental vibrational frequencies for water clusters, (H2O)(n), n = 2−5. *J. Phys. Chem. A* **2006**, *110* (1), 303−309.
(99) Kreinbihl, J. J.; Frederiks, N. C.; Waller, S. E.; Yang, Y.; Johnson, C. J. Establishing the structural motifs present in small ammonium and aminium bisulfate clusters of relevance to atmospheric new particle formation. *J. Chem. Phys.* **2020**, *153* (3), 034307.
(100) Knorke, H.; Li, H.; Liu, Z. F.; Asmis, K. R. Vibrational spectroscopy of the hexahydrated sulfate dianion revisited: role of isomers and anharmonicities. *Phys. Chem. Chem. Phys.* **2019**, *21* (22), 11651−11659.
(101) Alecu, I. M.; Zheng, J.; Zhao, Y.; Truhlar, D. G. Computational Thermochemistry: Scale Factor Databases and Scale Factors for Vibrational Frequencies Obtained from Electronic Model Chemistries. *J. Chem. Theory Comput.* **2010**, *6* (9), 2872−87.
(102) Temelso, B.; Morrell, T. E.; Shields, R. M.; Allodi, M. A.; Wood, E. K.; Kirschner, K. N.; Castonguay, T. C.; Archer, K. A.; Shields, G. C. Quantum Mechanical Study of Sulfuric Acid Hydration: Atmospheric Implications. *J. Phys. Chem. A* **2012**, *116* (9), 2209−2224.
(103) Temelso, B.; Phan, T. N.; Shields, G. C. Computational Study of the Hydration of Sulfuric Acid Dimers: Implications for Acid Dissociation and Aerosol Formation. *J. Phys. Chem. A* **2012**, *116* (39), 9745−9758.

https://doi.org/10.1021/acs.jpca.1c05466
J. Phys. Chem. A 2021, 125, 8454−8467

(104) Luchini, G.; Alegre-Requena, J. V.; Funes-Ardoiz, I.; Paton, R. S. GoodVibes: automated thermochemistry for heterogeneous computational chemistry data. *F1000Research* **2020**, *9*, 291.
(105) Ren, L.; Bai, H.; Yu, X.; Wu, F.; Yue, S.; Ren, H.; Li, L.; Lai, S.; Sun, Y.; Wang, Z.; et al. Molecular composition and seasonal variation of amino acids in urban aerosols from Beijing, China. *Atmos. Res.* **2018**, *203*, 28−35.
(106) Seinfeld, J. H.; Pandis, S. N. *Atmospheric Chemistry and Physics: From Air Pollution to Climate Change*; John Wiley & Sons, Inc.: Hoboken, NJ, 2016.
(107) Husar, D. E.; Temelso, B.; Ashworth, A. L.; Shields, G. C. Hydration of the Bisulfate Ion: Atmospheric Implications. *J. Phys. Chem. A* **2012**, *116* (21), 5151−5163.
(108) Morrell, T. E.; Shields, G. C. Atmospheric implications for formation of clusters of ammonium and 1−10 water molecules. *J. Phys. Chem. A* **2010**, *114* (12), 4266−71.
(109) Bustos, D. J.; Temelso, B.; Shields, G. C. Hydration of the Sulfuric Acid-Methylamine Complex and Implications for Aerosol Formation. *J. Phys. Chem. A* **2014**, *118* (35), 7430−7441.
(110) Kildgaard, J. V.; Mikkelsen, K. V.; Bilde, M.; Elm, J. Hydration of atmospheric molecular clusters: a new method for systematic configurational sampling. *J. Phys. Chem. A* **2018**, *122* (22), 5026−5036.
(111) Alongi, K. S.; Dibble, T. S.; Shields, G. C.; Kirschner, K. N. Exploration of the potential energy surfaces, prediction of atmospheric concentrations, and prediction of vibrational spectra for the HO2 (H2O)n (n = 1−2) hydrogen bonded complexes. *J. Phys. Chem. A* **2006**, *110* (10), 3686−3691.
(112) Kirschner, K. N.; Hartt, G. M.; Evans, T. M.; Shields, G. C. In search of CS2(H2O)(n = 1−4) clusters. *J. Chem. Phys.* **2007**, *126* (15), 154320.
(113) Hartt, G. M.; Shields, G. C.; Kirschner, K. N. Hydration of OCS with one to four water molecules in atmospheric and laboratory conditions. *J. Phys. Chem. A* **2008**, *112* (19), 4490−5.
(114) Elm, J. Clusteromics I: Principles, protocols, and applications to sulfuric acid-base cluster formation. *ACS Omega* **2021**, *6*, 7804−7814.
(115) Elm, J. Clusteromics II: Methanesulfonic acid-base cluster formation. *ACS Omega* **2021**, *6*, 17035−17044.
(116) Shields, G. C. Twenty years of exceptional success: The molecular education and research consortium in undergraduate computational chemistry (MERCURY). *Int. J. Quantum Chem.* **2020**, *120*, No. e26274.

https://doi.org/10.1021/acs.jpca.1c05466
J. Phys. Chem. A 2021, 125, 8454−8467